Factors Determining Vesicular Lipid Mixing Induced by Shortened Constructs of Influenza Hemagglutinin

Danika L. LeDuc,[‡] Yeon-Kyun Shin,*[,‡] Raquel F. Epand,[§] and Richard M. Epand[§]

Department of Chemistry, University of California−Berkeley, Berkeley, California 94720, and Department of Biochemistry, McMaster University Health Sciences Center, 1200 Main Street West, Canada ON L8N 3Z5

Received October 22, 1999; Revised Manuscript Received December 16, 1999

ABSTRACT: The HA2 subunit of influenza hemagglutinin is responsible for fusion of the viral and host-cell membranes during infection. An N-terminal 127 amino acid construct of HA2, FHA2−127, is shown to induce lipid mixing of large unilamellar vesicles under endosomal low pH conditions. Thus, FHA2 could serve as a good model system for biophysical studies of membrane fusion. With FHA2, we began to develop a mechanistic model which could explain how this short construct facilitates membrane fusion. In this endeavor, we studied the possible role of the kinked loop region (amino acids 105−113). A construct missing this loop, FHA2−90, although able to induce lipid mixing, has lost the sharp pH-dependent transition seen with FHA2−127 and native HA. In addition, FHA2−127 promotes extensive vesicle aggregation more effectively than FHA2−90 upon acidification. These data suggest that the kinked loop may play a pH-dependent regulatory role. To test this, we compared bis-ANS binding to the two constructs and observed that binding to FHA2−127 increases at a faster rate than FHA2−90 as the pH is decreased, indicating that the kinked loop not only is an ANS-binding site, but that it binds better at low pH. The pH dependence of this transition directly correlates with that observed in lipid mixing. Further, cysteine mutations of acidic residues in the kinked region are both fusion inactive and bind much less ANS, whereas a similar mutation of a threonine residue had little effect on fusion activity or ANS binding. This evidence lends further support to our idea that the kinked loop serves a regulatory role. To test the physiological relevance of the FHA2−127 fusion mechanism, we studied the effects of a G1E mutation, known to abolish fusion in native HA. We found that G1E−127 is fusion inactive as expected. This evidence indirectly suggests that the mechanism of FHA2−127 is perhaps physiologically relevant and from its study, we can learn much about the mechanism of native HA.

Membrane fusion is ubiquitous, occurring in all life processes in which cellular contents must be passed through a membrane barrier, such as viral infection, neurotransmission, fertilization, and intracellular protein trafficking (for review, see ref *1*). Specialized membrane-bound proteins are often required to assist in overcoming the free-energy barriers to membrane fusion, such as water exclusion and membrane apposition. Recent structures of a variety of fusion proteins show a similar core structure, which suggests the possibility of a general mechanism of action (*2*, *3*). In a search for such a possible generality of the fusion mechanism, the hemagglutinin protein of the influenza virus is arguably the best model system.

Hemagglutinin is a glycosylated membrane protein which exists as a trimer on the surface of the influenza virus. HA[1] is posttranslationally cleaved to yield two chains, denoted HA1 and HA2, which remain linked by a disulfide bond. HA1 contains a binding site for its cell-surface receptor, sialic acid, which is attached to carbohydrates of host cell membrane proteins. After binding, the cell internalizes the virus by endocytosis. The acidic pH of the endocytic vesicle induces a large dramatic conformational change in HA which exposes the highly hydrophobic N-terminus of HA2, the fusion peptide. Following this event, HA2 promotes rapid membrane fusion and ultimately insertion of the viral genome into the host cell (*4*).

Our studies have focused on a small construct of the ectodomain of HA2, FHA2−127 (a.a. 1−127). This construct consists of the N-terminal fusion peptide, a coiled-coil domain, and a kinked loop region, in a conformation analagous to the low-pH HA2 fragment structure (*5*). The fusion peptide inserts into target membranes (*6*) resulting in perturbation of membrane structure (*7*). It has been previously shown that the isolated 20 amino acid N-terminal fusion peptide can induce lipid mixing at high concentrations of peptide at low pH conditions (*8*). This N-terminal segment of FHA2−127 appears essential for promoting membrane fusion, as a construct missing this region, SHA2 (a.a. 32−127), is virtually completely inactive in inducing lipid mixing (*9*). However, the potency of the isolated fusion peptide in

* To whom correspondence should be addressed. Phone: (510) 643-5507. Fax: (510) 643-1255.

[‡] University of California−Berkeley.

[§] McMaster University Health Sciences Center.

[1] Abbreviations: HA, hemagglutinin; FHA2−127, residues 1−127 of HA2; FHA2−90, residues 1−90 of HA2; a.a., amino acids; SHA2, residues 32−127 of HA2; EPR, electron paramagnetic resonance; LUV, large unilamellar vesicles; bis-ANS, 4,4′-dianilino-1,1′-binaphthyl-5,5′-disulfonic acid; DOPC, dioleoylphosphatidylcholine; DOPE, dioleoylphosphatidylethanolamine; QUELS, quasi-elastic light scattering; N-Rh-PE, *N*-(lissamine Rhodamine B sulfonyl) phosphatidylethanolamine; N-NBD-PE, *N*-(7-nitro-2,1,3,-benzoxadiazol-4-yl) phosphatidylethanolamine.

10.1021/bi992457v CCC: $19.00
Published on Web 02/17/2000

promoting lipid mixing is far less than that of FHA2−127 (*9*). A factor which likely contributes to the increased potency of FHA2−127 is the coiled-coil region which makes the molecule trimeric, allowing several fusion peptides to function together in a cooperative manner. The role, if any, of the kinked loop had not yet been determined. However, recent spin-labeling EPR studies of this region (a.a. 105−113) of FHA2−127 showed that acidification results in decreased solvent accessibility, but not membrane insertion, of these residues (*10*). Negatively charged at neutral pH, the kinked loop is perhaps more protonated under acidic conditions creating an exposed, hydrophobic patch. Adjacent FHA2−127 trimers may aggregate at these junctions allowing for even larger FHA2−127 clusters. Previous work has shown that for native HA, such aggregation of multiple trimers is necessary for fusion (*11*−*13*).

The present work extends our previous studies to determine the mechanism by which FHA2−127 causes lipid mixing. The structure of the soluble domain of FHA2−127 has been shown to be virtually the same as the low pH HA2-fragment structure (*14*). For FHA2−127, the membrane topology of the fusion peptide region has also been determined (*15*). In this work, we show that the kinked loop region plays a regulatory role in FHA2−127-induced fusion. Further, we show that a well-known G1E phenotype mutation blocks the FHA2-induced lipid mixing as it does in native HA. A mechanistic model for FHA2-induced membrane fusion consistent with experimental data is proposed. Since FHA2−127 causes membrane fusion assayed by lipid mixing, conclusions derived from FHA2−127 studies should be useful in understanding the mechanism of membrane fusion in general.

MATERIALS AND METHODS

Materials. The amino acid sequence of FHA2−90 from the X-31 strain of influenza virus is GLFGAIAGFIENGWEGMIDGWYGFRHQNSEGTGQAADLKSTQAAIDQINGKLNRVIEKTNEKFHQIEKEFSEVEGRIQDLEKYVEDTKID, and the full 127 amino acid FHA2 also has the additional residues LWSYNAELLVALENQHTIDLTDSEMNKLFEKTRRQLR at the carboxyl terminus. Mutants G1E−90 and G1E−127 were made by site-directed mutagenesis using the Quikchange Kit from Stratagene (Cedar Creek, TX). These peptides were expressed in *Escherichia coli* BL21(DE3)pACYC as previously described (*10*). Final peptide preparations were purified to approximately 98% purity in concentrations ranging from 40 to 100 μM in the following buffer: 0.05% Triton X-100, 500 mM NaCl, 0.4 mM DTT, 1 mM EDTA, 1 mM PMSF, and 5 mM citrate-phosphate buffer, pH 7.

All phospholipids as well as the fluorescently labeled lipids *N*-(lissamine Rhodamine B sulfonyl)phosphatidylethanolamine (N-Rh-PE) and *N*-(7-nitro-2,1,3-benzoxadiazol-4-yl) phosphatidylethanolamine (N-NBD-PE) were purchased from Avanti Polar Lipids (Alabaster, AL). The labeled lipids were made from egg phosphatidylcholine by transphosphatidylation. Other fluorescent labels were purchased from Molecular Probes (Eugene, OR).

Preparation of Large Unilamellar Vesicles (LUVs). Appropriate concentrations of lipids were dissolved in chloroform/methanol (2/1 v/v) and deposited on the walls of a glass tube by drying first under a stream of nitrogen and then for 2 h in a vacuum desiccator. Lipid films were then rehydrated with the appropriate buffer, vortexed and freeze thawed five times to produce a suspension containing 12.5 mg/mL lipid.

This suspension was then extruded 10 times through two 100 nm polycarbonate filters (Nucleopore, Pleasanton, CA) using a steel barrel extruder (Lipex Biomembranes, Vancouver, BC) under nitrogen pressure. After extrusion, LUVs were stored on ice under argon and used within a few hours.

Quasi-Elastic Light Scattering. The size distribution of the LUVs was determined with quasi-elastic light scattering using a Brookhaven model B1 9000AT digital correlator equipped with a BI-200sm goniometer, version 2.0, and a BI-900AT Digital Correlator System. Size distribution was calculated using a nonnegatively constrained least-squares method with software provided by the instrument manufacturer.

Lipid Mixing Assay for Membrane Fusion. The resonance energy transfer assay of Struck et al. (*31*) was used to monitor membrane fusion. LUVs were prepared from DOPC:DOPE:cholesterol at a molar ratio of 1:1:1. Two populations of LUVs were prepared, one unlabeled and one labeled with 2 mol % each of N-Rh-PE and N-NBD-PE. A 9:1 molar ratio of unlabeled to labeled liposomes was used in the assay. In a typical experiment, LUVs at a lipid concentration of 150 or 300 μM were added to 2 mL of buffer containing 5 mM Hepes, 5 mM Mes, 5 mM citric acid, 0.15 M NaCl, and 1 mM EDTA, pH 7.0 (Hepes-Mes-citrate), continuously stirred at 37 °C in a 1 cm^2 silanized glass cuvette. The peptide was then injected, and the fluorescence was recorded at pH 7. The pH of the sample was then brought down to 5.0 by adding a small volume of 1 M citric acid. After recording the fluorescence for several minutes, complete lipid mixing was induced by adding 20 μL of 10% Triton X-100. Fluorescence was recorded at excitation and emission wavelengths of 465 and 530 nm, respectively, using a 490 nm cutoff filter placed between the cuvette and the emission monochromator, with 4 nm bandwidths, on a SLM Aminco Bowman AB-2 spectrofluorimeter. The initial residual fluorescence intensity, F_o, was taken as zero. The maximum fluorescence intensity, F_{max}, was obtained by the complete dilution of labeled lipids by Triton X-100. The percent lipid mixing at time t is given by $[(F_t - F_o)/(F_{max} - F_o)]100$.

All of the assays reported here were repeated at least twice. The observed rate of lipid mixing was reproducible to within ±15% of the value measured at any particular time, for assays carried out with a single liposome preparation (used within a few hours of preparation) and a single peptide preparation. Measurements made with different liposome preparations on different days showed greater variability. The exact amounts of both Triton X-100 (TX), although less than 0.001% in all experiments, and aggregated or denatured protein in a protein preparation cannot be accurately established. Since TX inhibits the fusogenicity of these proteins and denatured or aggregated protein does not contribute to fusion, these factors complicate direct quantitative comparison of the constructs.

Leakage. Leakage of vesicle contents was measured according to the procedure of Ellens et al. (*32*). A solution containing 12.5 mM ANTS, 45 mM DPX, 68 mM NaCl, 5 mM Hepes, 5 mM Mes, and 5 mM citric acid was adjusted to pH 7.0. The osmolarity was adjusted to 335 mosm with NaCl, and measured with a cryoosmometer (Advanced Model 3MOplus Micro-Osmometer, Advanced Instruments

Inc., Norwood, MA). Lipid films were suspended in buffer containing the ANTS and DPX, at a lipid concentration of 12.5 mg/mL. LUVs were made by extrusion as described above and the unentrapped material separated by passing the extruded vesicles through a 2.5 × 20 cm column of Sephadex G-75 (Pharmacia, Sweden), eluting with Hepes-Mes-citrate buffer, pH 7.0, adjusted to 335 mosm. The LUVs eluted in the void volume (7 mL) and were kept on ice prior to use. The lipid concentration in this suspension was determined by phosphate analysis (*33*). Excitation and emission wavelengths were 360 and 530 nm, respectively. A 490 nm cutoff filter was placed between the cuvette and the emission monochromator, and 4 nm bandwidths were used. In a typical experiment, 300 or 150 μM LUVs were placed in a quartz cuvette containing 2 mL of buffer pH 7.0, at 37 °C. After the peptide was added, the fluorescence was recorded and then the pH was lowered to 5.0 by acidification with 1 M citric acid. After recording the fluorescence for several minutes, 20 μL of 10% Triton X-100 was added to obtain 100% leakage. The percent leakage at any time was calculated as for lipid mixing. Runs were done in duplicate and showed good agreement. Controls were done as in lipid mixing. No significant light scattering artifacts or detergent control-induced vesicle leakage were observed.

Bis-ANS Fluorescence. A solution of bis-ANS was added to 2 mL of a buffer of 5 mM Hepes, 5 mM Mes, 5 mM citric acid, 0.15 M NaCl, and 1 mM EDTA, pH 7.4 (Hepes-Mes-citrate), to give a final concentration of 3.2 μM bis-ANS. Peptides were added to the buffer prior to the bis-ANS, at a concentration of 0.125 μM for FHA2 and FHA2(1−90) and 1 μM for the mutant forms of FHA2. The mixture was incubated for 20 min to allow for equilibration. Fluorescence was measured using siliconized glass cuvettes, at 37 °C. Excitation was set at 400 nm and the emission was measured at 479 or 474 nm, with a 420 nm cut off filter placed between the cuvette and the emission monochromator. After measurement of the bis-ANS spectrum at neutral pH, the pH was lowered with the addition of small aliquots of 1 M citric acid. All measurements were done in duplicate. No changes in fluorescence emission intensity of bis-ANS were observed with pH in the absence of peptide.

RESULTS

The pH dependence of HA-mediated fusion is known to correspond to a dramatic conformational change in the protein at the initial stage of fusion. The pH 7 structure exhibits a buried fusion peptide, which is distant from both the target and viral membranes (*16*). At pH 5, the fusion peptide is exposed as it is displaced 100 Å by extension of the central coiled-coil (*5*). It has been hypothesized that HA is kinetically trapped in its pH 7 conformation and that low pH allows it to adopt a more thermodynamically stable state (*17*). The resulting free energy released during this process may somehow be used to dehydrate the intermembrane space of the lipid bilayers, although the precise mechanism for such a process has not been experimentally determined (*18*).

A similar mechanism cannot explain FHA2−127-mediated mixing of vesicles. In the absence of the HA1 subunit, the low pH conformation is expected to be attained even at neutral pH (*14*). Indeed, the central coiled-coil retains the extended trimeric structure with kinked loops in this shorter construct (*10, 19*). In addition, spin-labeling EPR experiments

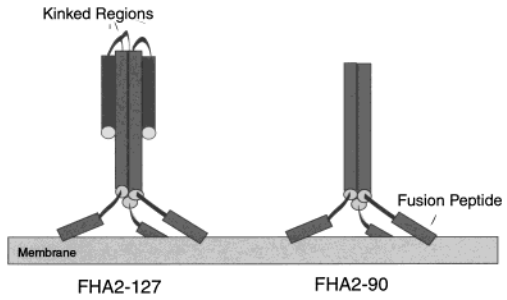

FIGURE 1: Structural models of FHA2−127 and FHA2−90 bound to a membrane.

indicate that the fusion peptide exists as a locally monomeric helix which inserts into the membrane at both neutral and fusogenic pH at approximately a 25° angle from the horizontal on the membrane surface (*20*) (Figure 1). Hence, in these respects, FHA2−127 has the structural appearance of the low pH form of HA, but without the loaded energy from a conformational change to aid in fusion. Yet, FHA2−127 still induces lipid mixing in LUVs under endosomal low pH conditions (*9*). This, along with the fact that FHA2−127 promotes lipid mixing far more effectively than the fusion peptide alone, demonstrates that other domains of FHA2−127 must contribute to the acceleration of lipid mixing.

This study attempts to elucidate what the functional role of the kinked loop region might be for FHA2−127-induced lipid mixing. The introduction of cysteine mutations at acidic residues in the kinked loop region abolishes the fusogenicity of FHA2−127, whereas a cysteine mutation at an adjacent threonine did not alter the extent or rate of lipid mixing (*9*). These data suggest that the kinked loop region must play a critical role in membrane fusion. Since the above results suggest that the overall charge of the kinked loop might be important in FHA2−127 fusogenicity, we performed ANS-binding studies to determine if the hydrophobicity of the kinked loop changes with a decrease in pH.

ANS-Binding Assays. The fluorescence probe bis-ANS does not fluoresce in aqueous solutions but becomes strongly fluorescent in a hydrophobic environment. This probe is often used to bind to hydrophobic surfaces of proteins where it undergoes an increase in quantum yield (*20*). Thus, the ability to bind ANS indicates an exposed hydrophobic site. (This binding is not necessarily indicative of membrane interaction.) Bis-ANS has been previously used with both the intact influenza virus (*21*) as well as the bromelain-cleaved ectodomain of the influenza hemagglutinin protein (*22*) to study the appearance of hydrophobic-binding sites at low pH. These studies both demonstrated an increase in bis-ANS binding to HA at acidic pH. This pH-dependent increase in ANS binding could be explained, of course, by the exposure of the hydrophobic fusion peptide at acidic pH, but could also indicate an increase in the hydrophobicity of other domains. We have employed this probe to study segments of the ectodomain of the HA2 subunit, FHA2−127. For FHA2−127, there is a large increase in the fluorescence of bis-ANS when the pH is changed from 7.4 to 4.6 (Figure 2). The steep pH dependence in ANS binding for FHA2−127 on lowering pH closely resembles what has been observed in the intact influenza virus (*21*).

We also examined the pH-dependence of the fluorescence of several cysteine mutants in the kinked loop region. These

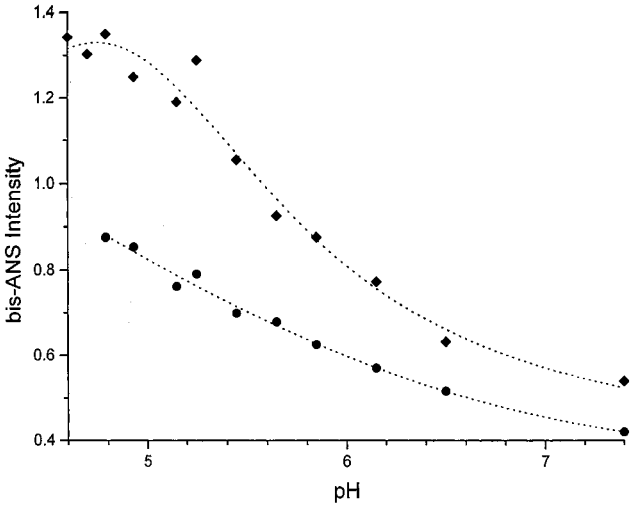

FIGURE 2: Fluorescence intensity of bis-ANS in the presence of FHA2−127 (diamonds) or FHA2−90 (circles) as a function of pH.

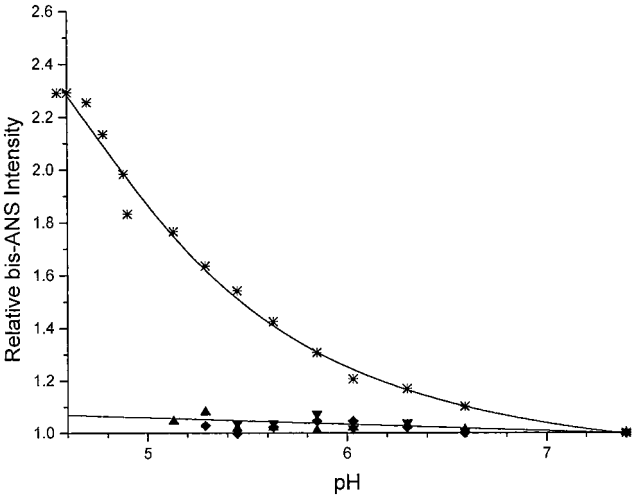

FIGURE 3: Relative fluorescence intensity of bis-ANS in the presence of (T111C)-FHA2 (*), (E114C)-FHA2 (diamonds), (D112C)-FHA2 (down arrows) or (D109)C-FHA2 (up arrows) as a function of pH. The absolute fluorescence intensity is lower than that of FHA2−127 for all of the Cys mutants. The different sensitivity to pH is best illustrated by showing the fluorescence intensity of the peptide at a particular pH relative to its value of pH 7.4.

constructs bound much less bis-ANS than the wild-type FHA2−127, and, for this reason, the mutant peptides, except for T111C, were studied at 8-fold higher concentration. It is particularly interesting that the pH dependence of the fluorescence for these mutants is largely maintained for the (T111C)-FHA2−127 but is completely lost with the other three mutants D109C, D112C, and E114C (Figure 3). Very interestingly, D109C, D112C, and E114C mutations of FHA2−127 have been determined to completely abolish lipid mixing under low pH conditions, while the T111C mutant retains the full fusogenicity of FHA2−127. The deletion of a negative charge in the loop may shift the pH necessary for titrating the remaining negatively charged residues lower. Thus, the pH-dependent exposure of hydrophobic-binding sites correlates very well with the fusogenic potency of these peptides (*9*). These results indicate that the kinked region is most likely one of the major binding sites for bis-ANS upon acidification and that there is an increase in the hydrophobicity of this region at low pH. This is consistent with earlier

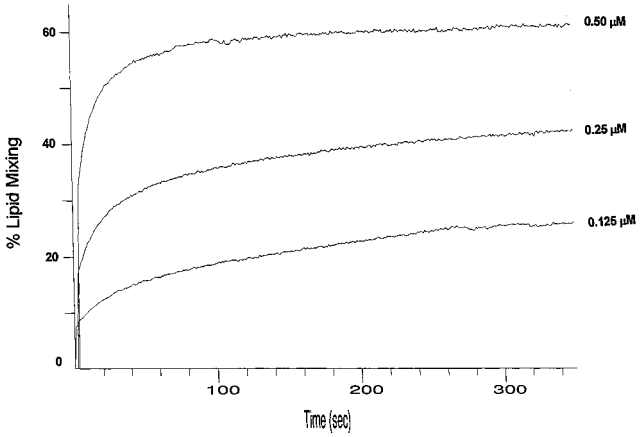

FIGURE 4: Promotion of lipid mixing by FHA2−90 of 150 μM LUVs of DOPC:DOPE:cholesterol (1:1:1) at pH 5.0, 37 °C. The curves represent lipid mixing observed in the presence of 0.50, 0.25, or 0.125 μM FHA2−90.

EPR studies which demonstrated that the kinked loops cause the aggregation of FHA2−127 trimers (*10*).

Deletion of the Kinked Loop. The close correlation between lipid mixing and bis-ANS binding could be indicative of some functional roles of the kinked loop in FHA2-induced membrane fusion. To determine its specific function, we compared the FHA2−127 lipid mixing assays and bis-ANS-binding studies with those of a shorter construct, FHA2−90, which is missing the kinked loop and subsequent helix. FHA2−90 does contain the fusion peptide and is trimeric as determined by glutaraldehyde cross-linking (data not shown). The measurements of fusion by lipid mixing and of liposome leakage were initiated by addition of peptide to a suspension of the liposomes in pH 7.0 buffer, followed by acidification to the desired pH. There is a marked increase in the rate of lipid mixing when LUVs of DOPC:DOPE:cholesterol (1:1:1) are acidified to pH 5 in the presence of FHA2−90 (Figure 4).

We can conclude that little, if any, lipid-mixing activity is lost at pH 5 by removal of the kinked loop in going from FHA2−127 to FHA2−90. However, when these data are compared with the previously reported results for FHA2-127, we see some distinct differences in the pH dependence. With regard to bis-ANS binding for FHA2−90, ANS binds much more weakly to FHA2−90 than to FHA2−127 at all pH conditions studied. This is most likely due to the lack of the putative ANS-binding loop in FHA2−90. Additionally, the increase in bis-ANS binding to FHA2−90 over the pH range 7.4−4.6 occurs more gradually as the pH is decreased than is seen with FHA2−127 (Figure 2). In lipid-mixing assays, both peptides exhibit a marked increase in fusogenic activity at acidic pH (Figure 5), but the pH dependence of FHA2−90 occurs over a broader range of pH and less closely resembles that of the virus than those of FHA2−127 (*23*). Thus, FHA2−90 is fusion active, but has lost the sharp, pH-dependent transition seen in native HA and FHA2−127.

Quasi-Elastic Light Scattering Experiments. We further compared the properties of FHA2−127 and FHA2−90 by measuring their effect on vesicle aggregation. The aggregation of LUVs of DOPC:DOPE:cholesterol (1:1:1) was measured by right angle light scattering as well as by turbidity measurements. At neutral pH, there is no time dependence of turbidity of the LUVs either with or without

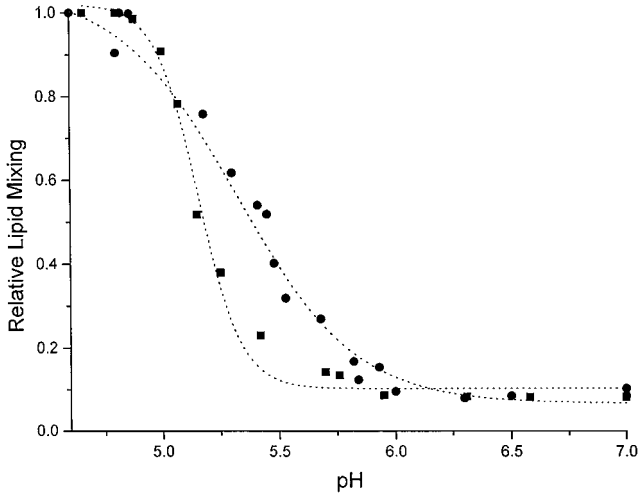

FIGURE 5: pH dependence of the effects on membrane fusion of 150 μM LUVs composed of DOPC:DOPE:cholesterol (1:1:1) with FHA2−90 (solid circles) or FHA2−127 (solid squares). The % lipid mixing as the value measured at each pH at 350 s, relative to that measured for each of the two peptides at pH 4.2. Rate of increase of lipid mixing becomes very slow after 350 s. Measurements were carried out with two different batches each of the constructs with 0.25 and 0.125 μM concentration in separate experiments.

added peptide. Upon acidification of LUVs alone, there is little change in the turbidity, but in the presence of FHA2−127 or FHA2−90, there is a time-dependent increase which is more rapid with FHA2−127 (data not shown). The vesicle aggregating properties of FHA2−90 were studied more extensively with quasi-elastic light scattering (QUELS) and compared with those of FHA2−127. In the absence of peptide, but with the same amount of detergent, analysis of the 100 nm diameter extruded vesicles showed that their size was close to that anticipated from the pore size of the polycarbonate filter and that they had a narrow size distribution. The size distribution did not change with either time or pH (data not shown). This was also the case after addition of FHA2−127 at pH 7 (Figure 6a). Acidification of the liposomes in the presence of FHA2 caused little change in the mean diameter but did broaden the size distribution over the first 10 min (Figure 6a). After 180−220 min, the distribution was bimodal, with a fraction of the vesicles having a size on the order of microns. Neutralization of this mixture markedly reduced the average size, although the size was still greater than the original vesicles (Figure 6a). Increased size of the vesicles can be caused by either aggregation of the vesicles or by membrane fusion. The partial reversibility of the size of the very large aggregates with pH demonstrates that they are formed mostly by aggregation (*10*), but the finding that the final size is larger than the initial vesicles after neutralization suggests that some vesicle fusion has taken place, in accord with the results of the lipid mixing assays. In comparison, FHA2−90 exhibits much less increase in size on incubation at pH 5 (Figure 6b). The initial mean diameter of the vesicles at pH 7 is somewhat larger in the presence of FHA2−90 and suggests there may already be extensive aggregation of the liposomes to dimers even at pH 7. This would be in accord with the observed leakage activity of this peptide at neutral pH (Figure 7). With time, the average size of the vesicles increases but there is no extensive aggregation, with the average size being close to that of three liposomes. The average size is somewhat reduced by neutralization back to pH 7, but this reversal in vesicle size is not as dramatic as with FHA2−127.

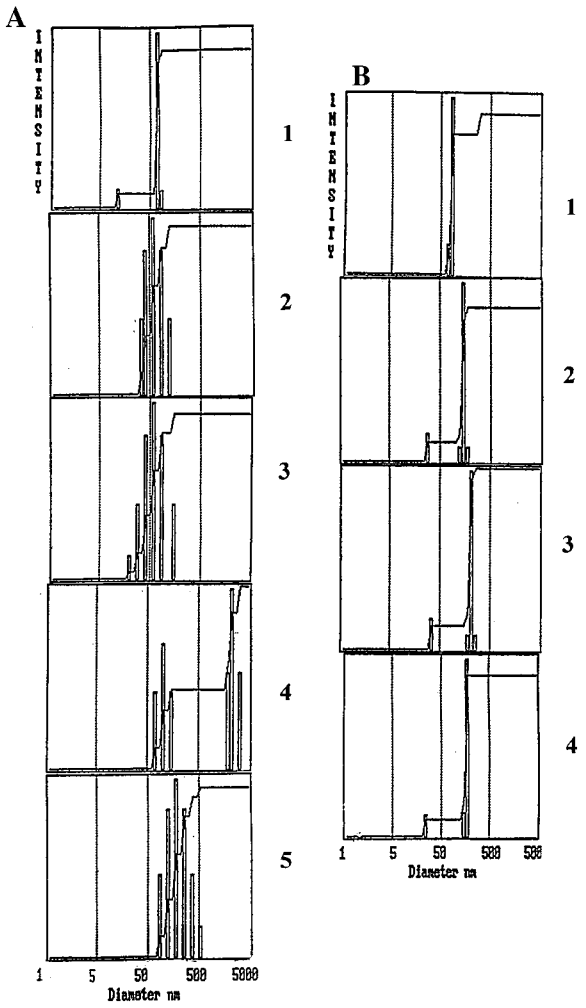

FIGURE 6: QUELS analysis of vesicle size distribution after incubation at 25 °C with 0.25 μM peptide: (a) FHA2−127, from top to bottom: curve 1, pH 7, "zero time"; curve 2, pH 5, "zero time"; curve 3, pH 5, 10 min; curve 4, pH 5, 220 min; curve 5, reneutralized to pH 7 at 220 min. (b) FHA2−90, from top to bottom: curve 1, pH 7, "zero time"; curve 2, pH 5, "zero time"; curve 3, pH 5, 180 min; curve 4, reneutralized to pH 7. LUVs (300 μM) of DOPC:DOPE:cholesterol (1:1:1) were used. The graphs show scattering intensity versus particle diameter on a logarithmic scale, assuming a spherical shaped particle. For "zero time" data, QUELS was measured immediately after sample preparation, but the resulting size distribution comes from data averaged over 5 min.

G1E Fusion-Inhibiting Mutation. We also tested the similarity of FHA2-mediated fusion to that induced by native HA by determining the effect of mutation on FHA2's lipid-mixing ability. It has been previously shown that a mutation at position 1 of HA2 from Gly to Glu in native HA abolishes fusion while nativelike interaction with lipid is retained (*24*). If FHA2−127-mediated fusion is physiologically relevant, such a mutation should also abolish lipid mixing activity in our in vitro vesicle system. Indeed, the G1E−127 mutant is unable to induce a significant amount of lipid mixing under low pH conditions (Figure 8). In addition, whereas FHA2−127 facilitated the aggregation of LUVs, the average vesicle size remained constant upon acidification when G1E−127 was added instead (data not shown). This provides additional evidence for the physiological relevance of the FHA2-induced lipid mixing.

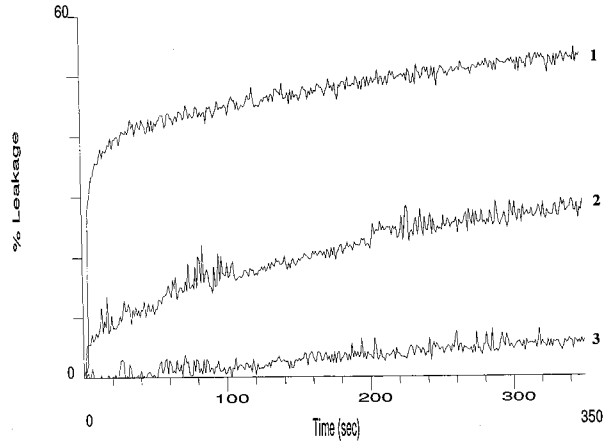

FIGURE 7: Promotion of vesicle contents leakage by FHA2−90 of 150 μM LUVs of DOPC:DOPE:cholesterol (1:1:1) at 37 °C. The curves represent vesicle contents leakage observed in the presence of 0.25 μM FHA2−90 after (curve 1) or before (curve 2) acidification. Leakage of LUV in the absence of peptide is shown in curve 3. See Materials and Methods section for details of the assay conditions.

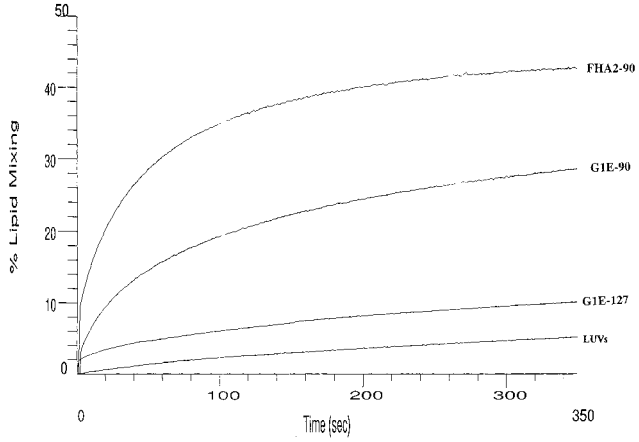

FIGURE 8: Comparison of lipid mixing induced by 0.125 μM FHA2−90, G1E−90, and G1E−127 with 75 μM LUVs of DOPC:DOPE:cholesterol (1:1:1) at pH 5.0, 37 °C.

In contrast, our results with G1E−90, the G1E mutant for FHA2−90, suggest that FHA2−90 can cause lipid mixing by means of a different mechanism. Although there is again some decrease in lipid mixing upon making the mutation, G1E−90 is still approximately 70% as effective in inducing lipid mixing and about three times as effective as G1E−127. Further, the QUELS data show a moderate increase in the mean diameter of vesicle aggregates upon acidification with G1E-90, which is partially reversed upon bringing the solution to pH 7 (data not shown). This result suggests that the peptide is somehow destabilizing the membrane and causing lipid transfer.

DISCUSSION

The details of the molecular mechanism by which viral proteins promote membrane fusion is largely unknown. At a minimum, the fusion protein must bring together the viral envelope and target membrane as well as perturb the bilayer arrangement in the target membrane. Comparing the present results of lipid mixing assays with FHA2−127 and FHA2−90 with earlier work done with SHA2 (a.a. 32−127) and the fusion peptide, we can conclude that the fusion peptide and coiled-coil region are necessary components for membrane fusion (*9*). Hence, FHA2−90 possesses most of the components required to promote rapid lipid mixing of liposomes under low pH conditions.

It had been shown that bis-ANS binds to influenza virus in a pH-dependent manner (*21*). The low-pH-induced hydrophobic exposure assayed by bis-ANS binding could contribute to the pH dependence of the binding of hemagglutinin protein to membranes and to the pH dependence of the acceleration of membrane fusion. The similarity of bis-ANS binding to FHA2−127 and the intact virus suggests that FHA2−127 contains the region responsible for the hydrophobic ANS-binding site. A role in membrane fusion for this ANS-binding site is indicated by the strong correlation between amount of ANS binding and ability to induce lipid mixing among the FHA2−127 mutants studied: those binding less ANS also are less effective in inducing pH-regulated lipid mixing. Thus, as with fusion, FHA2−127 has a steeper pH dependence of bis-ANS binding than FHA2−90. Also, FHA2−127 binds more bis-ANS than FHA2−90. In addition, the only Cys mutant of four in the kinked loop region which exhibits pH-dependent binding of bis-ANS, (T111C)-FHA2−127, is also the only Cys mutant in this region of the peptide which promotes membrane fusion. A pH-dependent increase in bis-ANS binding could be due to either a pH-induced conformational change, which exposes a hydrophobic site or the titration of an already exposed surface. Our data indicate that the kinked region is most likely an ANS-binding site since (1) there is less ANS binding to FHA2−90 and (2) Cys mutations of acidic residues in this region greatly affect ANS-binding. The kinked region is already exposed in FHA2−127, so a likely explanation for the increase in bis-ANS binding is the titration of acidic residues with a decrease in pH. Thus, the kinked region seems to serve as a pH-regulated switch, perhaps inhibiting fusion at neutral pH by preventing trimer clustering and accelerating it at pH 5 by facilitating the same trimer clustering through hydrophobic interactions.

The important regulatory role of the kinked loop region and the helix following it is further evidenced by results obtained from the G1E mutants of FHA2−127 and FHA2−90. G1E-127 behaves in a manner expected of HA2 in the native virus and shows little lipid mixing or vesicle aggregation. Surprisingly, G1E-90 retains most of its lipid mixing function and induces vesicle aggregation upon acidification, albeit somewhat less than that observed with FHA2−90. A possible explanation for this unexpected behavior could be that FHA2−90 can induce lipid mixing through a different mechanism than either FHA2−127 or native HA. Our lipid mixing studies with the G1E mutants imply that such a mechanism might require a hydrophobic region that is present in FHA2−90 but not in FHA2−127 to interact with the membrane. Since this requirement exludes the fusion peptide, another hydrophobic region must be present. In addition to the kinked loop, FHA2−90 is also missing the short helical segment which binds to the outside of the main coiled-coil (Figure 1). Thus, the C-terminal end of the coiled-coil is exposed in FHA2−90 and not in FHA2−127. Without the outer helices, a relatively hydrophobic face becomes exposed as indicated in the crystal structure (*5*). This new nonpolar face could interact with the membrane or the hydrophobic fusion peptide from nearby trimers. Although this is highly

speculative, reinspection of our bis-ANS-binding data provides some support for this speculation. The removal of a single acidic residue from the kinked loop in the FHA2−127 mutants D109C, D112C, and E114C reduced ANS binding to approximately 1/8 of that observed with FHA2−127 at neutral pH. FHA2−90, which is missing the entire kinked loop, would be expected to bind this same reduced amount, or even less, of ANS, but instead binds approximately 1/2 that of FHA2−127, indicating the presence of an alternative ANS-binding site.

FHA2−90 perhaps induces lipid mixing through a mechanism in which the C-terminal end of the coiled-coil, in addition to the fusion peptide, interacts with the membrane. Thus, the kinked loop appears to play a regulatory role in membrane fusion by preventing leakage at neutral pH and other mechanisms of lipid mixing.

A mechanistic model of FHA2−127-mediated membrane fusion begins to develop from interpreting this and other data. The coiled-coil region would allow the formation of a trimeric structure which would contain three fusion peptides. It would act by focusing the fusion peptides to the membranes. Considering that the fusion peptide is the only region interacting with membranes in our model system, it is conceivable that these N-terminal segments could facilitate membrane adhesion by inserting into different membranes from one trimer. The kinked loop could bring these adjacent trimers together. The kinked loop may also facilitate the tilting of the trimers (*25*). The energy from this hydrophobic interaction may be transferred into water exclusion, allowing for membrane apposition.

The present work focuses on the features of HA, which facilitate membrane fusion, and more specifically, the mechanistic steps between the pH-induced conformational change through lipid mixing. The mechanism of action of FHA2−127 most likely parallels that of the GPI-anchored ectodomain of HA which is known to only promote hemifusion (*26*, *27*). Pore formation and content mixing require the transmembrane domain, and without the HA1 subunit we cannot look at such aspects as receptor binding and the nature of the conformational change. Further, our simplified system does not contain all the factors of a biological membrane which may affect membrane fusion.

Thus, development of a membrane fusion model for FHA2−127 may not translate directly to a complete model for native HA. For instance, we observe that even though FHA2−127 has already assumed the low pH, fusion-competent conformation, it still requires acidic pH to proceed with lipid mixing. Previous work with native HA shows that a conformational change induced by low pH, urea, or heat is enough to allow membrane fusion to proceed at pH 7, 37 °C (*28*−*30*). The effect of urea or high temperature on the structure of HA has not been well characterized. The possibility exists that these conditions may induce less than optimal rates of fusion through alternative pathways.

Although we have obtained some indirect evidence that FHA2−127 may be biologically relevant, it appears that a cellular fusion assay using FHA2−127 is necessary to confirm this. Yet, the parallels that have been observed between it and the native virus, such as pH-dependent lipid mixing and ANS binding, clearly demonstrate that FHA2−127 is a minimal system from which we can learn a great deal about the general process of membrane fusion.

REFERENCES

1. White, J. M. (1992) *Science 258*, 917−924.
2. Weissenhorn, W., Dessen, A., Calder, L. J., Harrison, S. C., Skehel, J. J., and Wiley, D. C. (1999) *Mol. Membrane. Biol. 16*, 3−9.
3. Poirier, M. A., Xiao, W., Macosko, J. C., Chan, C., Shin, Y.-K., and Bennett, M. K. (1998) *Nat. Struct. Biol. 5*, 765−769.
4. Hernandez, L. D., Peters, R. J., Delos, S. E., Young, J. A., Agard, D. A., and White, J. M. (1997) *J. Cell Biol. 139*, 1455−1464.
5. Bullough, P. A., Hughson, F. M., Skehel, J. J., and Wiley, D. C. (1994) *Nature* 371, 37−43; Carr, C. M., and Kim, P. S. (1993) *Cell 73*, 823−832.
6. Durrer, P., Galli, C., Hoenke, S., Corti, C., Glück, R., Vorherr, T., and Brunner, J. (1996) *J. Biol. Chem. 271*, 13417−13421.
7. Colotto, A., and Epand, R. M. (1997) *Biochemistry 36*, 7644−7651.
8. Lear, J. D., and DeGrado, W. F. (1987) *J. Biol. Chem. 262*, 6500−6505.
9. Epand, R. F., Macosko, J. C., Russell, C. J., Shin, Y.-K., and Epand, R. M. (1999) *J. Mol. Biol. 286*, 489−503.
10. Kim, C.-H., Macosko, J. C., and Shin, Y.-K. (1998) *Biochemistry 37*, 137−144.
11. Blumenthal, R., Sarkar, D. P., Durell, S., Howard, D. E., and Morris, S. J. (1996) *J. Cell Biol. 135*, 63−71.
12. Danieli, T., Pelletier, S. L., Henis, Y. I., and White, J. M. (1996) *J. Cell. Biol. 133*, 559−569.
13. Ellens, H., Bentz, J., Mason, D., Zhang, F., and White, J. (1990) *Biochemistry 29*, 9697.
14. Chen, J., Wharton, S. A., Weissenhorn, W., Calder, L. J., Hughson, F. M., Skehel, J. J., and Wiley, D. C. (1995) *Proc. Natl. Acad. Sci. U.S.A. 92*, 12205−12209.
15. Macosko, J. C., Kim, C.-H., and Shin, Y.-K., (1997) *J. Mol. Biol. 267*, 1139−1148.
16. Wilson, I. A., Skehel, J. J., Wiley, D. C. (1981) *Nature 289*, 366−373.
17. Carr, C. M., and Kim, P. S. (1993) *Cell 73*, 823−832.
18. Koslov, M. M., and Chernomordik, L. V. (1998) *Biophys. J. 75*, 1384−1396.
19. Yu, Y. G., King, D. S., and Shin, Y.-K. (1994) *Science 265*, 274−276.
20. Rosen, C. G., and Weber, G. (1969) *Biochemistry 8*, 3915−3920.
21. Korte, T., and Herrmann, A. (1994) *Eur. Biophys. J. 23*, 105−113.
22. Bethell, R. C., Gray, N. M., and Penn, C. R. (1995) *Biochem. Biophys. Res. Commun. 206*, 355−361.
23. Doms, R. W., Helenius, A., and White, J. (1985) *J. Biol. Chem. 260*, 2973−2981.
24. Gething, M. J., Doms, R. W., York, D., and White, J. (1986) *J. Cell Biol. 102*, 11−23.
25. Tatulian, S. A., Hinterdorfer, P., Baber, G., and Tamm, L. K. (1995) *EMBO J. 14*, 5514−5523.
26. Kemble, G. W., Daniele, T., and White, J. M. (1994) *Cell 76*, 383−391.
27. Ruigrok, R. W., Aitken, A., Calder, L. J., Martin, S. K., Skehel, J. J., Wharton, S. A., Weis, W., and Wiley, D. C. (1988) *J. Gen. Virol. 69*, 2785−95.
28. Melikyan, G. B., White, J. M., and Cohen, F. S. (1995) *J. Cell Biol. 131*, 679−691.
29. Carr, C. M., Chaudhury, C., and Kim, P. S. (1997) *Proc. Natl. Acad. Sci. U.S.A. 94*, 14306−14313.
30. Schoch, C., Blumenthal, R., and Clague, M. J. (1992) *FEBS Lett. 311*, 221−225.
31. Struck, D. K., Hoekstra, D., and Pagano, R. E. (1981) *Biochemistry 20*, 4093−4099.
32. Ellens, H., Bentz, J., and Szoka, F. C. (1985) *Biochemistry 24*, 3099−3106.
33. Ames, B. N. (1966) Assay of inorganic phosphate, total phosphate and phosphatases. in *Methods in Enzymology* (Neufeld, E. F., and Ginsburg, V., Eds.) Vol. VIII, pp 115−118, Academic Press, New York.

BI992457V